Journal of Oceanography & Marine Environmental System 4 (2): 29-42, 2020
ISSN 2222-1395

DOI: 10.5829/idosi.jomes.2020.29.42

Mapping and Monitoring of Rosetta Promontory Shoreline Pattern Change, Egypt

[1]Sherif H. Balbaa, [1]Ayman A. El-Gamal, [2]Ahmed S. Mansour and [2]Mohamed A. Rashed

[1]Marine Geology Department, Coastal Research Institute (CoRI),
National Water Research Center (NWRC), Alexandria, Egypt
[2]Geology Department, Faculty of Science, Alexandria University,
Baghdad Street, Moharam Bek, Alexandria, Egypt

Abstract: The coastal strip of the Nile Delta has been suffering extensive erosion and accretion problems. This was achieved after the construction of many water regulation structures across the Egyptian part of the Nile River as dams and barrages, particularly the Aswan High Dam. In order to cease these problems several engineering hard structures have been built, but they translocated the problem to the adjacent sites. The aim of this study is to analyze the shoreline change pattern over a three decades temporal scale during the period between 1985 to 2015 along the coastal strip of Rosetta Promontory and the impact of these protective structures on the coastal area. Also, this study is to estimate the relation between the coastal changes and physical properties of the coastal sediments. This was accomplished by the automated delineation of the successive shorelines covering this period using remote sensing imagery by the MNDWI index. The extracted shorelines were manipulated through the Digital Shoreline Analysis System software. The study revealed that Rosetta Promontory has suffered from erosion with maximum shoreline retreat -137 m/y during the study period at the eastern sector of the promontory before the construction of the seawall. Over the past thirty years, the shoreline change rates were compared with sediments grain size, heavy minerals content and radioactivity of recent marine sediment samples. This comparison indicated that as the erosion increases, the heavy minerals content and radioactivity of the coastal sediments increases and vice versa.

Key words: Rosetta promontory · Remote sensing · Coastal area changes · Grain size · Heavy minerals · radioactivity

INTRODUCTION

The Nile Delta is one of the oldest deltaic systems in the world, which was formed since the Miocene [1]. It has great socioeconomic importance to the Egyptian country as it holds the biggest section of the population and possesses large agricultural and industrial facilities and fisheries. The coastal area of the Nile Delta suffered intensive processes of reorientation. The shoreline has been continuously changing due to different coastal processes as erosion, accretion and land subsidence. These changes were caused mainly due to anthropogenic activities. These activities involved the control structures over the Nile River. Different barrages and dams were established on the Nile River to control the water flow in Egypt. These are Delta barrage established in 1861, Assuit barrage in 1902, Esna barrage in 1908, Edfina Barrage in 1950, Aswan Low Dam in 1902 and Aswan High Dam in 1964 [2]. The Aswan High Dam and the other human structures across the Nile River have quantitatively reduced the amount of sediment flux carried by the Nile River to the Mediterranean Sea. The trapping effect of the High Dam is estimated to be about 98%, meaning that nearly all of the sediment stays in Lake Nasser and upstream of the Dam while only few sediment including silt and clay pass to the downstream [3]. Rosetta Promontory is the area that is mostly affected by these processes. Various studies have been proposed to discuss the alterations of the Rosetta Promontory. Some of these studies analyzed the historical maps [4, 5, 6] and others have utilized satellite images to delineate shorelines [7, 8, 9]. Several studies estimated the shoreline change rates [10, 11, 12] and others studied the effect of hard structures on the orientation of Nile Delta shoreline [13, 14, 15, 16].

Corresponding Author: Ayman A. El-Gamal, Marine Geology Department, CoRI, NWRC, 15 El-Pharaana Street, El Shallalat, Postal Code 21514, Alexandria, Egypt. Tel: +201005296027.

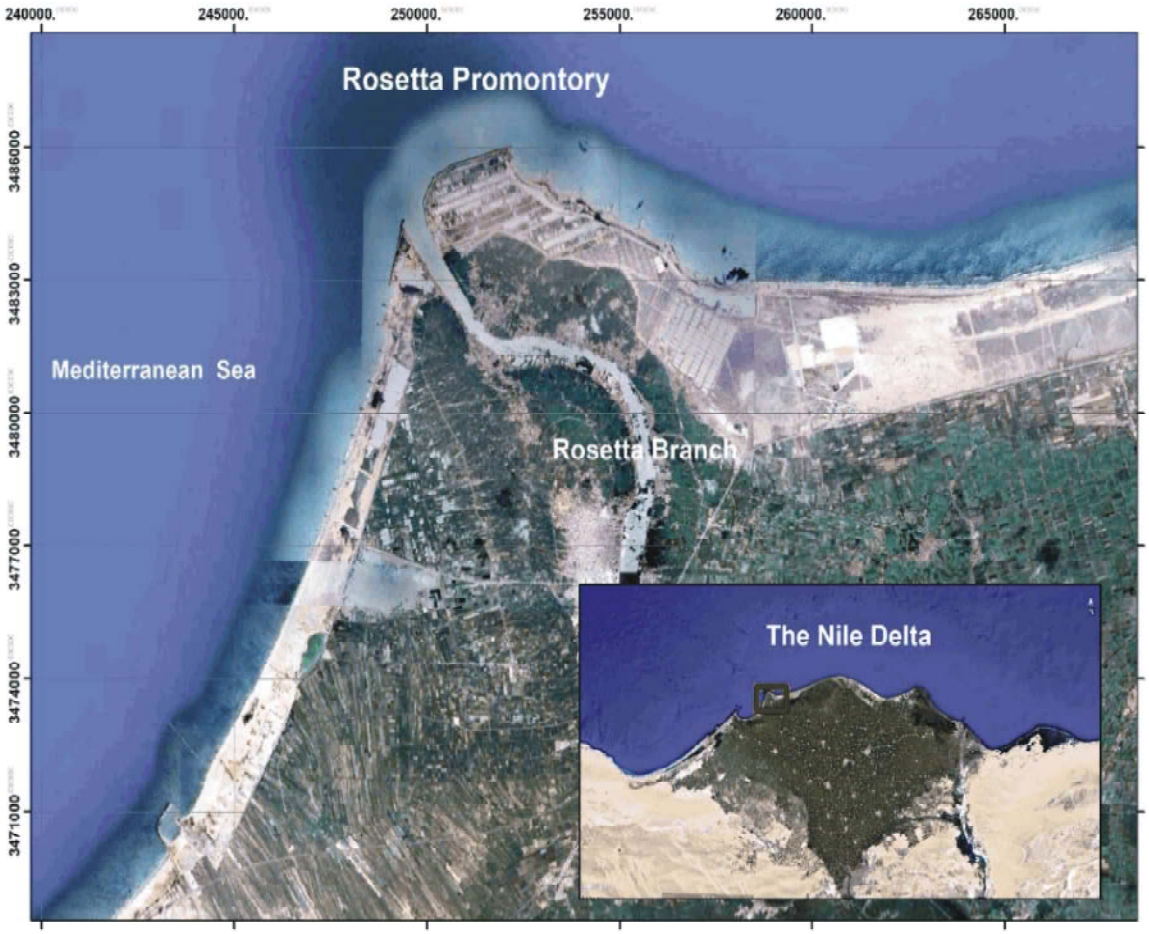

Fig. 1: Rosetta Promontory Location

Study Area

History and Overview: The Rosetta Promontory is located at northwestern area of the Nile Delta (Fig. 1). It lies on the eastern terminal of Abu-Qir Bay and at a distance of about 60 km east of Alexandria City. The old Canopic and Sebennitic Nile branches have been diverted to form the present Rosetta Branch from 500 to 1000 AD [17]. Rosetta promontory continued deposition and growing up till the beginning of the 20th century where it reached about 14 km towards the sea [18]. Then the regression process began after the construction of Aswan Low Dam (Fig. 2) in 1902 [19]. Many approaches tried to estimate the rate of shoreline change along the Rosetta Promontory. According to Fanos and his group [19], the Rosetta Promontory shoreline has retreated 4.4 and 5.8 km at the eastern and western sides, respectively during the period between 1900 and 1991. Ghoneim stated that the Rosetta Promontory, between 1972 and 2003, has lost about 9.5 km^2 of its ground area with shoreline retreating amount of 3 km [20]. The highest erosion rate calculated was 137 m/year [2]. The Rosetta Promontory problem could be summarized as the lack of sediment flux carried by the Nile water due to the construction of dams and barrages (specially the Aswan High Dam), that lead to the erosion problem that decrease the land area near the coastal zone. It has affected the socio-economic state at the promontory as agricultural, industrial and fishing facilities. Also, the accretion problem that leads to the siltation of the inlets and navigation channels that leads to the shoaling of the exits and deterioration of the fishing, navigation and ecosystem of the Rosetta area. This study aims to estimate the shoreline change rates during the period between 1985 to 2015 and the effect of the protective structures on these rates. Also, the work is to assess the relation among the shoreline changes, mean grain size distribution, heavy minerals concentrations and radioactivity.

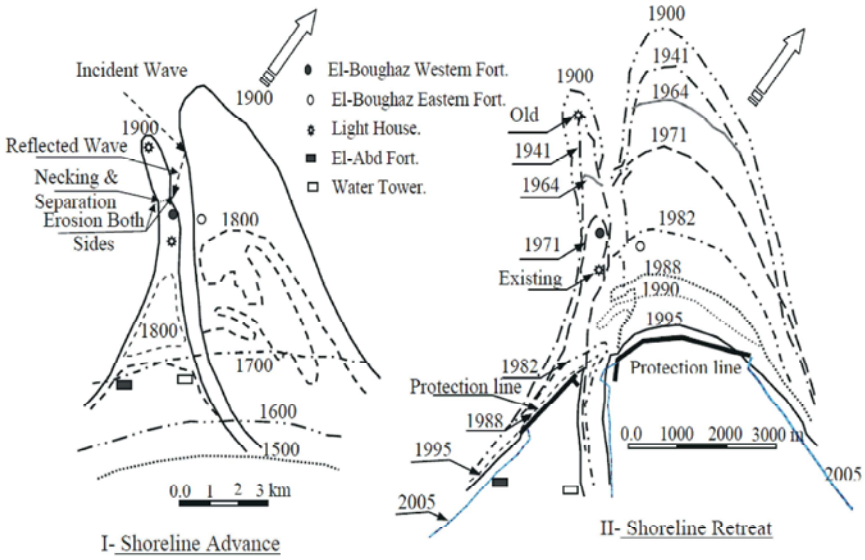

Fig. 2: Rosetta Promontory shoreline evolution since 1500 [17]

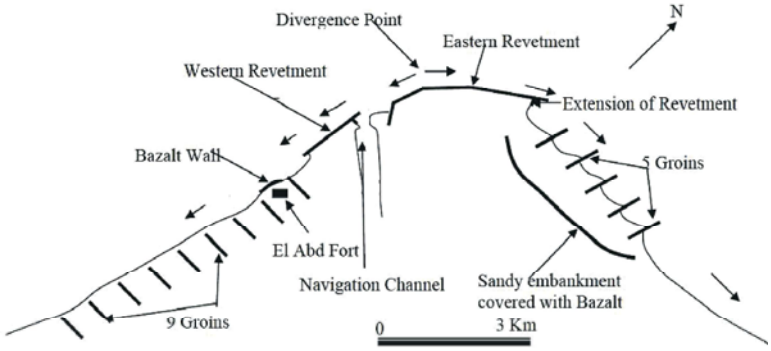

Fig. 3: Protection measures at Rosetta promontory [17]

Coastal Structures: Protective engineering structures have been executed to face the erosion and accretion problems of Rosetta promontory as revetments and groins (Fig. 3). Within the period between 1986 to 1991 two revetments (sea walls) of 1.5 and 3.5 km has been constructed inland at the western and eastern sides of Rosetta promontory, respectively [21]. The sea wall has armor weight 4 to 7 tons, 6.75 m high and 48 to 70 m wide [22]. The land before these revetments were eroded due to the wave and current actions and the lack of sediments supply to the promontory. After the construction of the two revetments, the two structures have actually stopped the retreat of the promontory shoreline but the erosion did not stop but continued vertical [23]. In 1998 the eastern revetment was extended a distance about 250 meters and 5 rubble mound groins were constructed inland to protect a distance of about 5 km on this side from intensive erosion. In 2000 around 40 short rubber-tube submerged groins were constructed at the southern side of the western revetment to protect a distance of 2 km but they failed and were destroyed and a basalt wall was constructed to protect local structures as El-Abd Fort. Also, between 2003 and 2005, to combat erosion rates, 15 groins were distributed at the eastern and western sides of the Rosetta Promontory sea walls including 5 groins with 400 to 500 m long and 800 to 900 m spacing distance [24].

MATERIALS AND METHODS

Shorelines Positions Delineation and Analysis: Seven images from Landsat including different sensors (MSS, TM, ETM+ and OLI) at unequal time intervals between 1972 and 2015 were exploited in this study to extract the shoreline positions. The shorelines were extracted using Erdas Imagine software. They were analyzed to estimate the change rates of the coastal line during the study period. The images were chosen taking

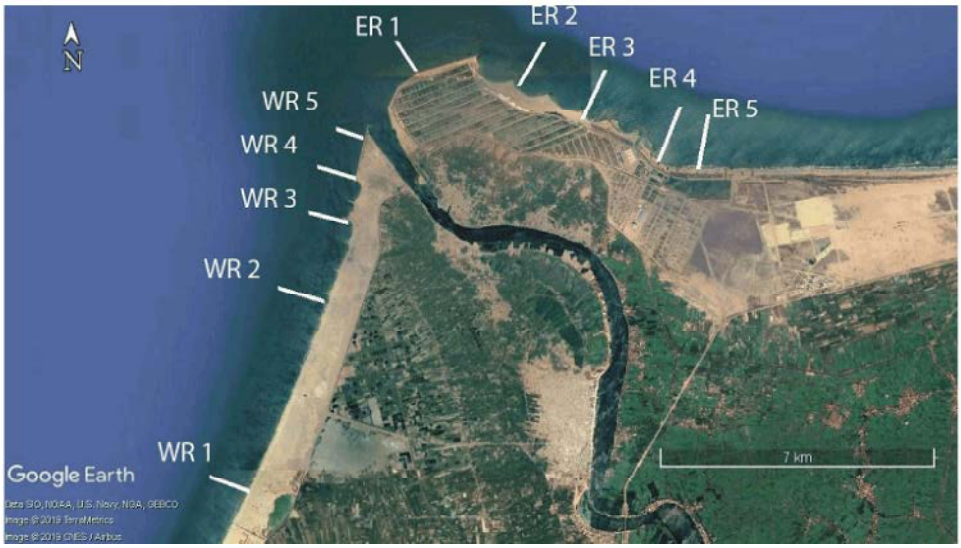

Fig. 4: Cross shore profiles of collected sediment samples

into consideration the cloud coverage percent and the dates of protective measures construction to study its effect. The shorelines were extracted using the Modified Normalized Difference Water Index (MNDWI), which was proposed by Xu [25]. It is calculated by:

$$\frac{Green - MIR}{Green + MIR}$$

where GREEN is a band that encompasses reflected green light, while MIR is a middle infrared band. The MNDWI was chosen to be the best index for automated shoreline mapping based on its performance with comparison with other seven Landsat water indices [26]. The vector data of the shorelines was obtained by using the ArcGIS software. Then it was reformatted and smoothed. The rates of shoreline change were estimated using the Digital Shoreline Analysis software (DSAS). DSAS uses a measurement baseline method to calculate rate-of-change statistics for a time series of shorelines. The DSAS analysis was used to establish transect locations and calculate the related change statistics.

Sedimentology: Recent sediment samples were collected from ten profiles across the study area. Their historical data were acquired from the Coastal Research Institute (CoRI) database. They were studied along with the shoreline change rates to demonstrate the relation between them. The recent sediment samples were analyzed for their mean grain size, heavy minerals concentrations and radioactivity. The profiles were nearly perpendicular to the shoreline at uneven spacing (Fig. 4). The profiles extend seaward to a 6 meters water depth or total profile distance of 1400 meters, which of them is closer. Each profile includes the beach sample and another 4 to 6 samples nearshore. The sediment samples were collected using Van Veen Grap Sampler. The samples were taken to the laboratory, washed by distilled water to remove salts and then dried to be ready for grain size analysis. This is done either by sieve analysis or wet pipette analysis. To carry out sieving analysis, a representative dry sand sample of the sediment were fetched and run through a set of sieves at one-phi (ϕ) interval to segregate the sample into subset size classes and weighing the amount of material retained on each sieve. The ϕ value is calculated as following:

$$\phi = -\log_2 D\,(mm)$$

where D is the grain diameter in millimeter.

For finer silt and clay grains, the wet pipette analysis method was conducted to determine the weight gradient of smaller grain diameters.

Heavy Minerals Analysis and Radioactivity Measurement: The heavy minerals in recent sediment samples are separated and weighted to determine its concentration in each sample. Bromoform was used in the present study to extract the heavy minerals portion by a procedure mentioned by Krumbein and Pettijohn [27]. The finer fractions only of each sample were obtained by sieving the sample and performing the heavy minerals

separation from only 3ϕ and 4ϕ portions [19]. After the extraction of the heavy portion of minerals from the sediment samples, the concentration was calculated in weight percentages relative to the original weight of sample. The gross radioactivity was measured for each sample of the recent ones using survey meter model SEI USB Inspector. The device includes a Geiger-Muller (GM) tube to detect radiations. It was calibrated using a standard radioactive sources of Cs-137 and Co-60 [28].

Results and Discussion

Shoreline Changes on the Temporal Scale: Fig. 5 shows the positions of the shorelines of Rosetta Promontory from 1985 to 2015 and their reorientation pattern. In this study the promontory was subdivided into two sectors; the western and the eastern sectors.

Western Rosetta Sector: The western sector in this study extends for nearly 14 km westward from the Rosetta mouth. This area included structures the western Rosetta revetment (1990) and western nine groins (2005). The sector shoreline were subdivided into four intervals; 1985 to 1990 (before revetment construction), 1990 to 2005 (before western groins), 2005 to 2010 (after western groins) and 2010 to 2015 to study the effect of groins on extended period. The estimated shoreline change rates are demonstrated in the Figures 6a to 6d. There are major variations in the change rates between the different time periods. This is due to the effect of the sediment trapping by the Aswan High Dam and afterwards the effect of the protective structures. During the first interval (between 1985 to 1990), the highest erosion rate was focused at the tip of the promontory (reaches nearly -39 m/y). The erosion rate decreases westward and tend to accretion at some transects. Then, from 1990 to 2005, the western seawall was constructed, the erosion rate at the tip of the promontory has nearly ceased except for the rest of the sandy body in front of the seawall itself (-1.9 m/y). Nevertheless, the western leeside of the structure has suffered relatively high erosion rate nearly -20 to -28 m/y. The erosion rate decreases westward till it turns to slight accretion at the west most region of the study area. In the next time intervals, the leeside of the western seawall has exhibited instability. The nine groins built at this sector has converted these high erosion rates to much less. This happens by the effect of the groins that stop the littoral current carrying sediment load, causing the drop of this load at the updrift side of the groin (accretion) and deficiency of sediment supply at the down drift side (erosion).

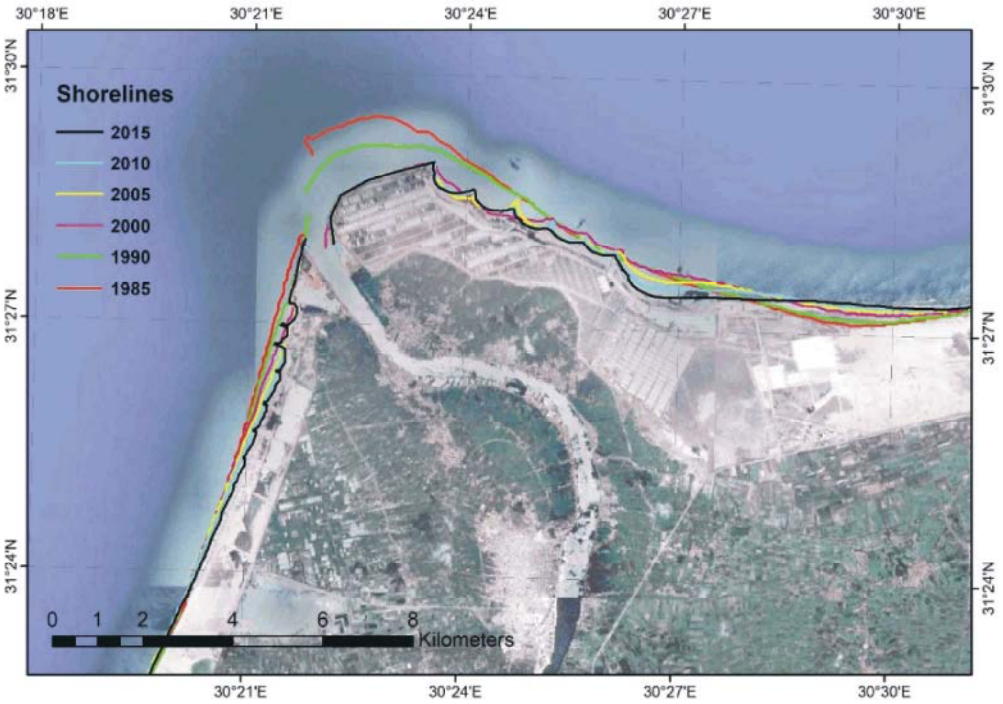

Fig. 5: Rosetta Promontory shorelines (1985 to 2015)

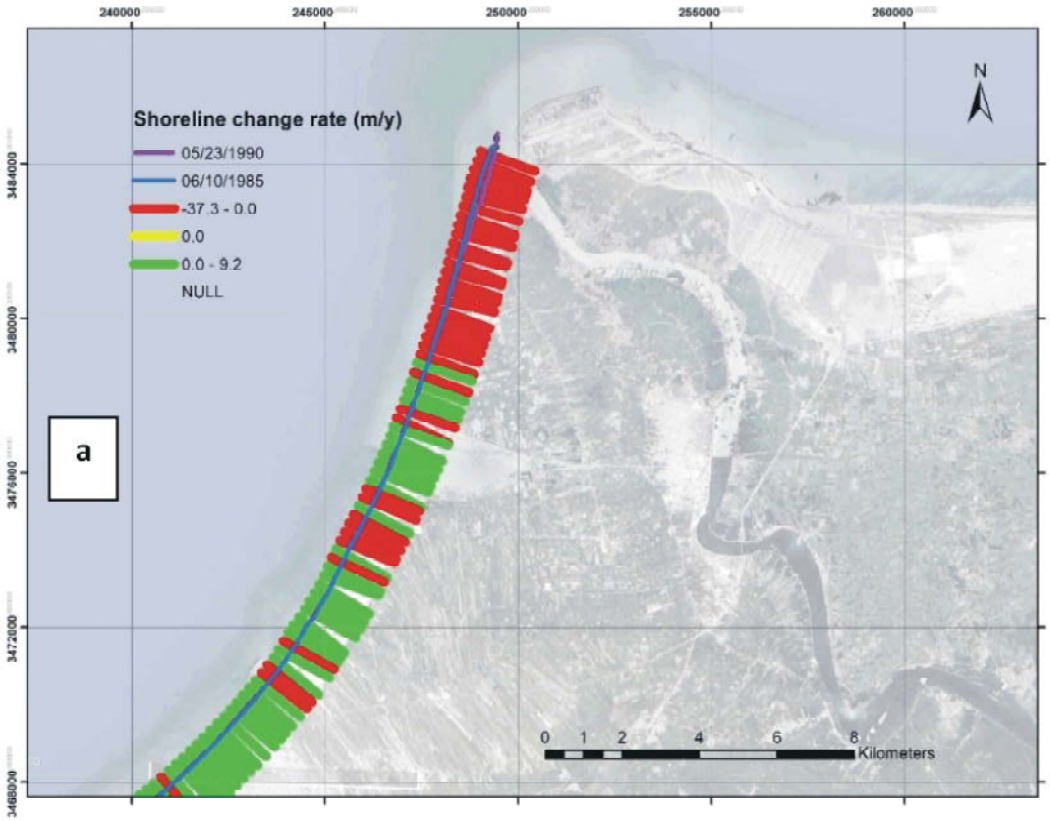
240000
245000
250000
255000
260000
N
Shoreline change rate (m/y)
05/23/1990
06/10/1985
-37.3 - 0.0
0.0
0.0 - 9.2
NULL
a
0 1 2 4 6 8
Kilometers

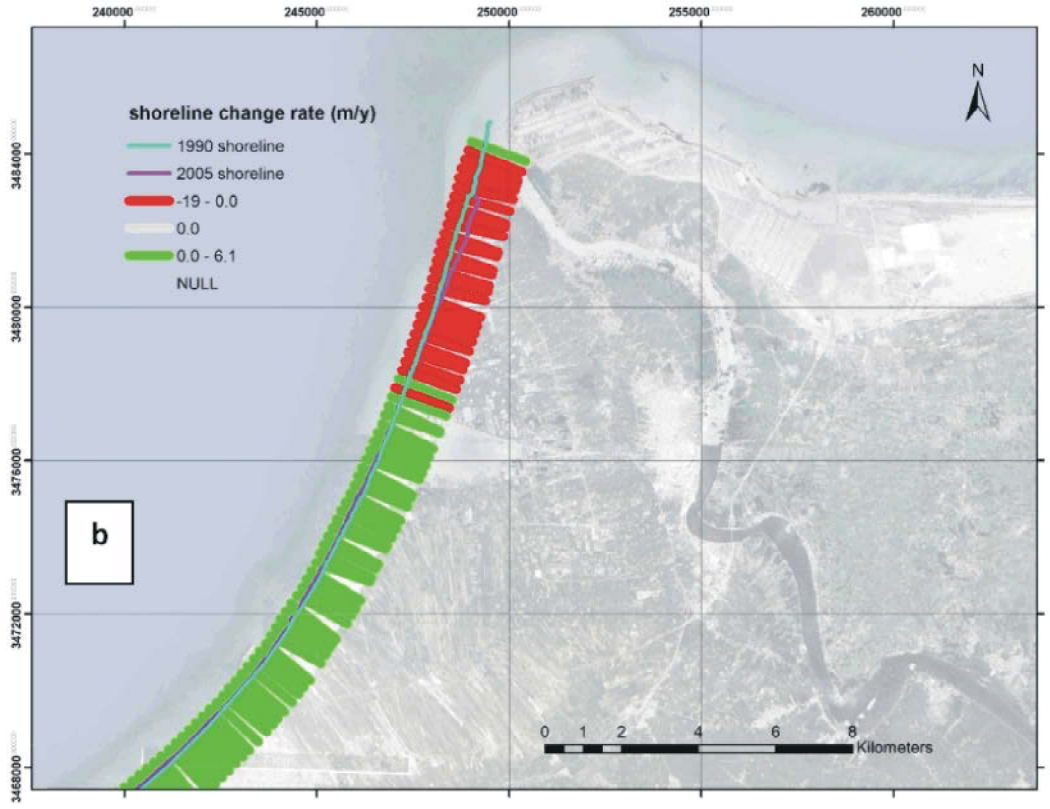
240000
245000
250000
255000
260000
N
shoreline change rate (m/y)
1990 shoreline
2005 shoreline
-19 - 0.0
0.0
0.0 - 6.1
NULL
b
0 1 2 4 6 8
Kilometers

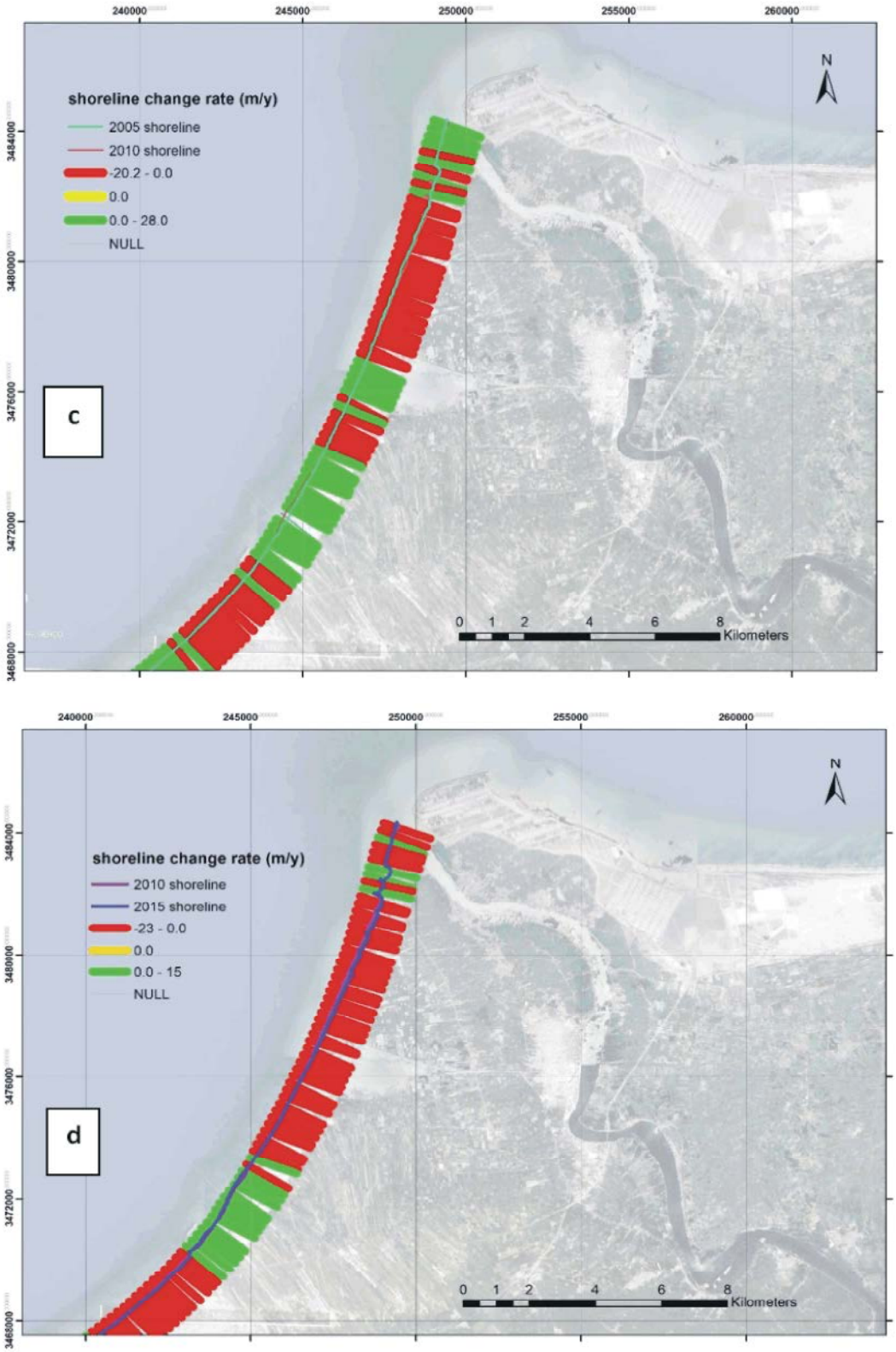

Fig. 6: Shoreline change rates at the western side of Rosetta Promontory at time intervals between: a) 1985 to 1990b) 1990 to 2005 c) 2005 to 2010 d) 2010 to 2015

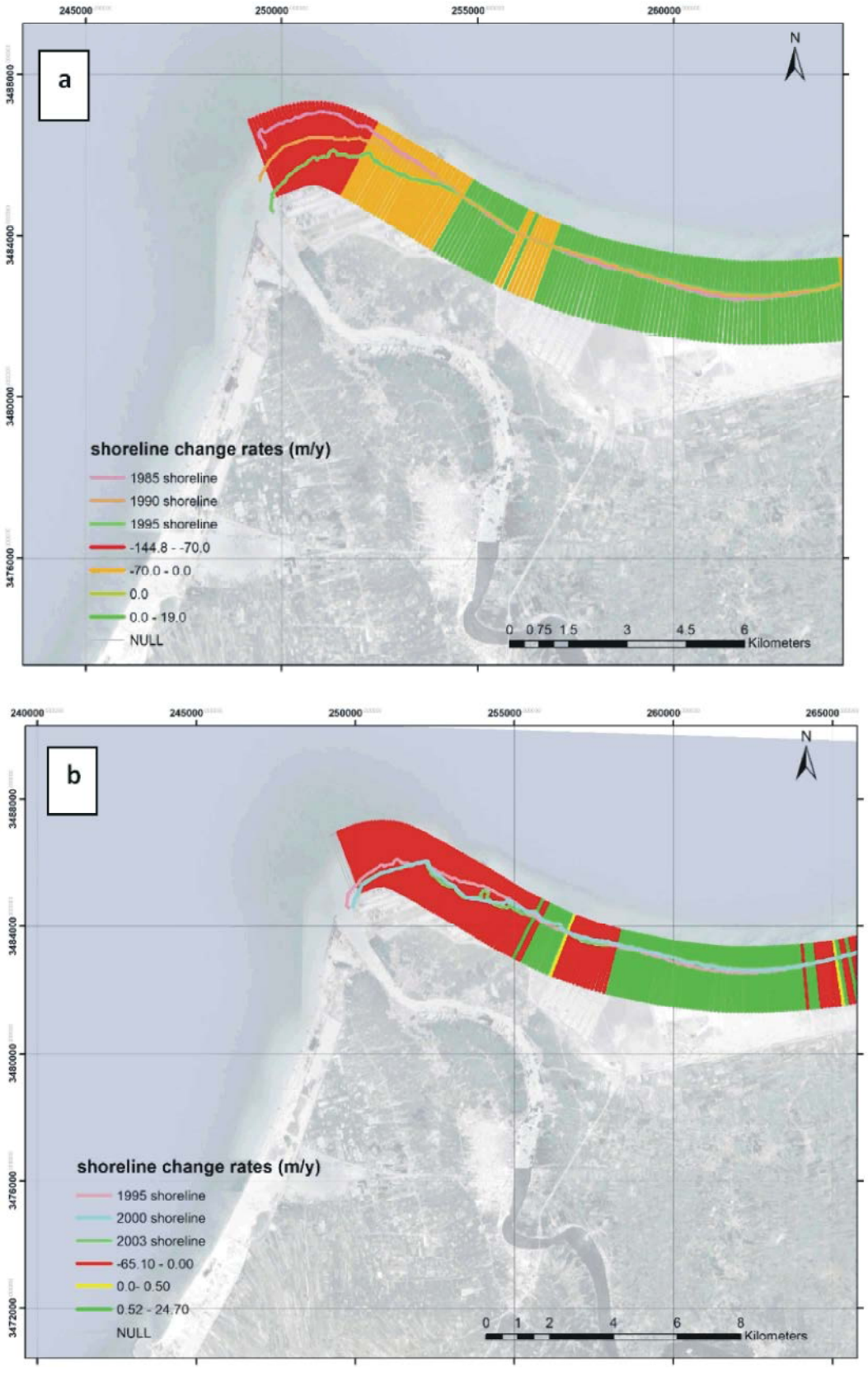
a
N
245000
250000
255000
260000
3488000
3484000
3480000
3476000
shoreline change rates (m/y)
1985 shoreline
1990 shoreline
1995 shoreline
-144.8 - -70.0
-70.0 - 0.0
0.0
0.0 - 19.0
NULL
0 0.75 1.5 3 4.5 6 Kilometers
b
N
240000
245000
250000
255000
260000
265000
3488000
3484000
3480000
3476000
3472000
shoreline change rates (m/y)
1995 shoreline
2000 shoreline
2003 shoreline
-65.10 - 0.00
0.0- 0.50
0.52 - 24.70
NULL
0 1 2 4 6 8 Kilometers

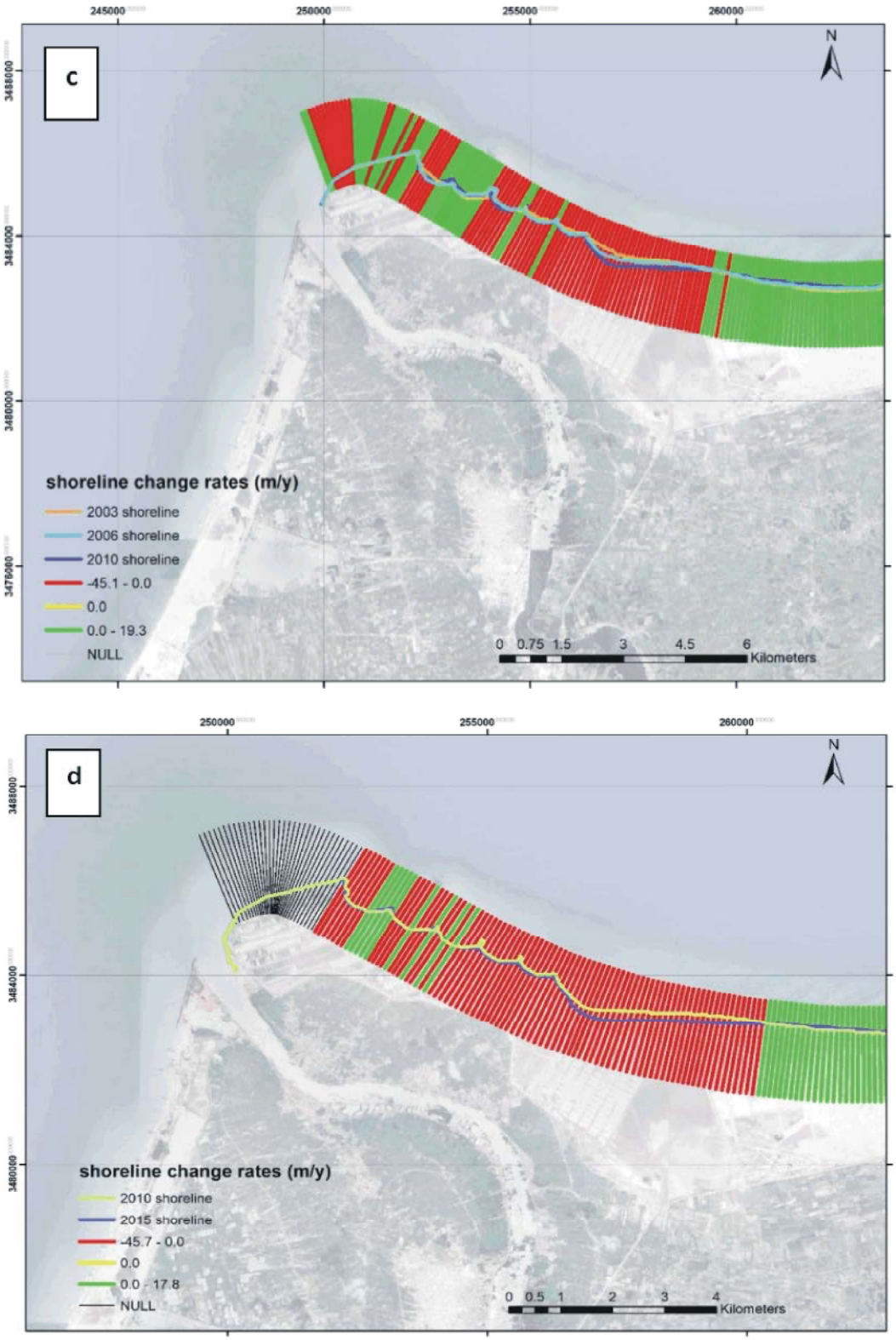

Fig. 7: Shoreline change rates at the eastern side of Rosetta Promontory at time intervals between: a) 1985 to 1995b) 1995 to 2003 c) 2003 to 2010 d) 2010 to 2015

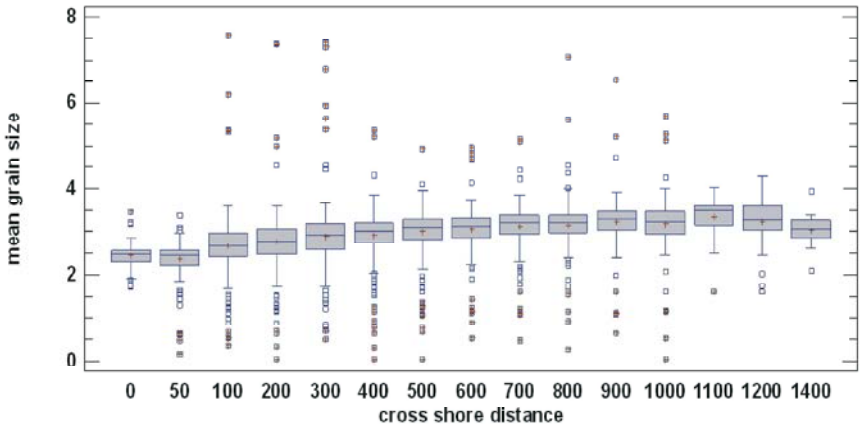

Fig. 8: Sediments grain size (in ϕ) variation along shore distance (in meters)

Eastern Rosetta Sector: The eastern sector extends for nearly 15 km eastward from the Rosetta mouth. This area includes the structures eastern Rosetta seawall and eastern five groins. Great variations dominate among the rates of erosion and accretion between the different time spans and the protective measures play the key role. The sector was divided into different time intervals to show the effect of the structures. Figures 7a to 7d demonstrates the change rates of the shoreline positions at this sector. Between 1985 and 1995; the Rosetta promontory tip suffered the most intensive erosion rate in the whole study area. The rate of erosion reaches nearly -138m/y. The erosion rate decreases gradually eastward till achieving accretion at the most eastern part of the study area. While between 1995 and 2003, after the construction of the Rosetta Eastern Seawall, the erosion at the tip has ceased except for the residual land infront of the revetment (-32 m/y). The erosion problem extended eastward to the lee side of the revetment with a rate reaches -64 m/y. The rate of erosion decreases eastward until turning to accretion with rate reaches 23 m/y eastward. During the next intervals, the effect of the five eastern groins appeared through decreasing or stopping the erosion rate at the updrift side and displacing the problem to the down drift side.

Grain Size Characteristics

General Grain Size Distribution among the Whole Study Area Between 1985 to 2015: The general grain size distribution among the study area shows that the mean grain size is finer at the promontories' tips and gets coarser away from the Rosetta outlet. This result was confirmed by Frihy and Lotfy work [19]. The distribution also showed that the grain size fining trend along with increasing the distance cross shore (Fig. 8). This fining trend provides some indication of sediment transport towards the offshore, which was mentioned by Frihy and Dewidar [8].

Grain Size Change During the Studied Time Intervals: The construction of the protective measures had played a key role in the redistribution of grain size along the coastal area. This can be emphasized by studying the grain size characteristics during different time spans before and after the construction process.

West Rosetta Promontory Sector: Figure 9 shows the distribution of the mean grain size along the western Rosetta Promontory studied profiles over the different time intervals. The intervals are divided according to the protective structures as follows: T1 between 1985 to 1990 (before construction of seawall), T2 between 1990 to 2005 (before construction of nine groins) and T3 between 2005 to 2015 (after the construction of seawall and groins). Profile WR1 shows some fining at T2 and T3 due to the erosion that took place after the hard structures' construction. WR 2 shows variations in mean grain size values, this sector of the shoreline was affected by relatively high erosion rates during the different time periods as it lies at the downdrift side of the seawall and at the western groins sector. At profile WR3 the mean grain size underwent continuous fining due to the continuous erosion during the successive time spans. This also was noticed in profiles WR4 and WR5, which were affected only by the seawall. The continuous fining at these two profiles is due to the scouring (vertical erosion) in front of the seawall as described by Frihy and his group [24].

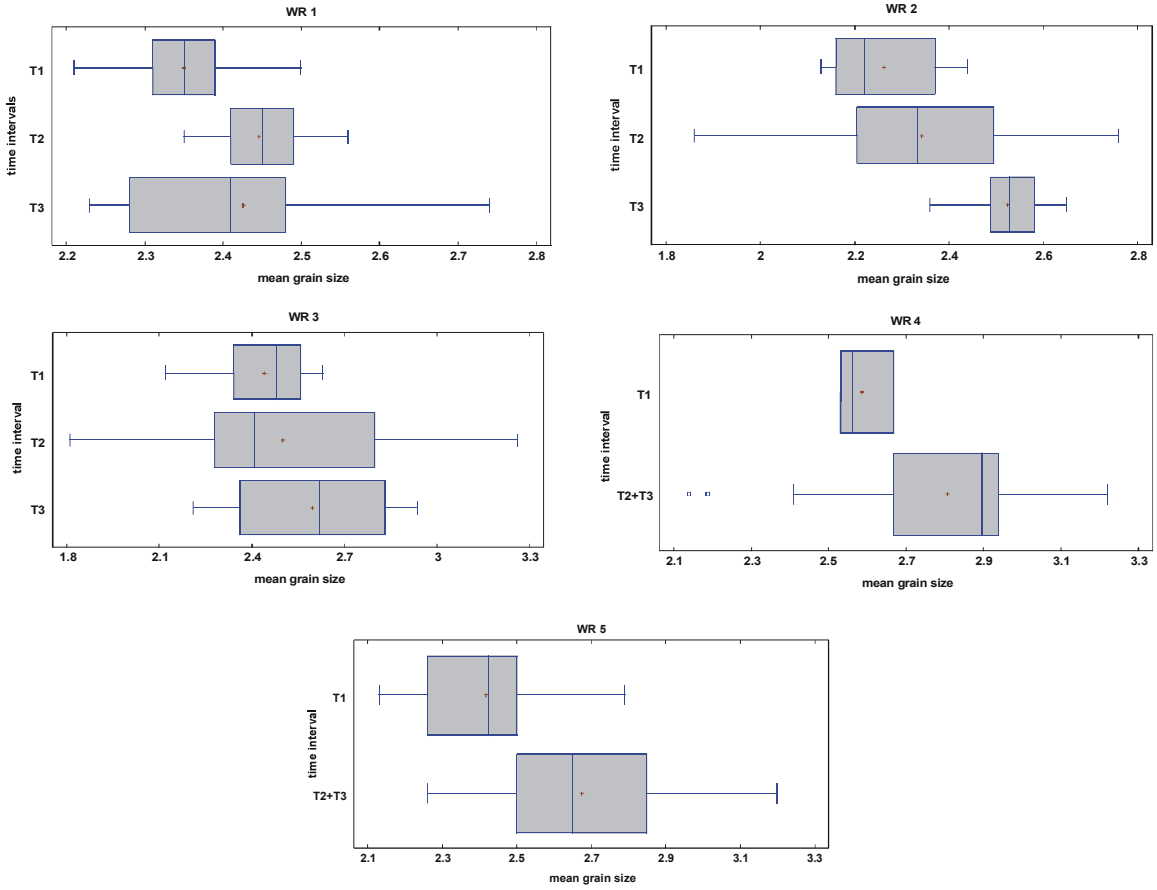

Fig. 9: The distribution of mean grain size among west Rosetta profiles WR 1, WR 2, WR 3, WR 4 and WR 5 over the different time spans

East Rosetta Promontory Sector: Figure 10 shows the distribution of grain sizes at East Rosetta Promontory profiles over different time spans according to the construction of the protective structures at this sector. The periods are between 1985 to 1995 (before the construction of the seawall) noted as T1, 1995 to 2003 (after the seawall effectiveness) noted as T2 and 2003 to 2015 noted as T3 (after the groins construction). Profile ER 1 is represented by only 2 periods of time as it lies at the Eastern revetment and only affected by its construction. It shows the fining of the mean grain size from the pre- and post-construction periods due to the continuous erosion at this sector. At profiles ER2 and ER 3, during T2, the grain sizes are fining due to erosion, while during T3, the grains were mixed with coarser grains due to slight accretion. Profiles ER 4 and ER 5 shows great fining in grain sizes as it suffered erosion after construction of the revetment and the groins. These values of grain sizes show compatibility with the values of shoreline change rates.

Heavy Minerals Concentrations and Radioactivity in the Sediment Samples: The heavy minerals concentrations show spatial variation along the study area and show a pattern relative to the shoreline change. It is obvious that the heavy minerals are enriched in coastal strips that suffered erosion (as the promontory tip). It relatively decreases in areas of accretion. By comparing the heavy minerals concentrations at each sample with the mean grain size value, radioactivity and shoreline change pattern, it appeared that there is a relation among them. Erosional beaches showed a fining trend in mean grain size, an increase in the heavy minerals concentrations and radioactivity, and vice versa. This pattern is due to the selective removal for the light minerals that is relatively coarser in grain size (as quartz and feldspar) and delivering them to the accretionary beaches leaving behind the finer denser heavy minerals increasing it concentration. This effect was mentioned in the work of different scientists [19, 29, 16]. The heavy minerals such as zircon and monazite have mineralogical composition

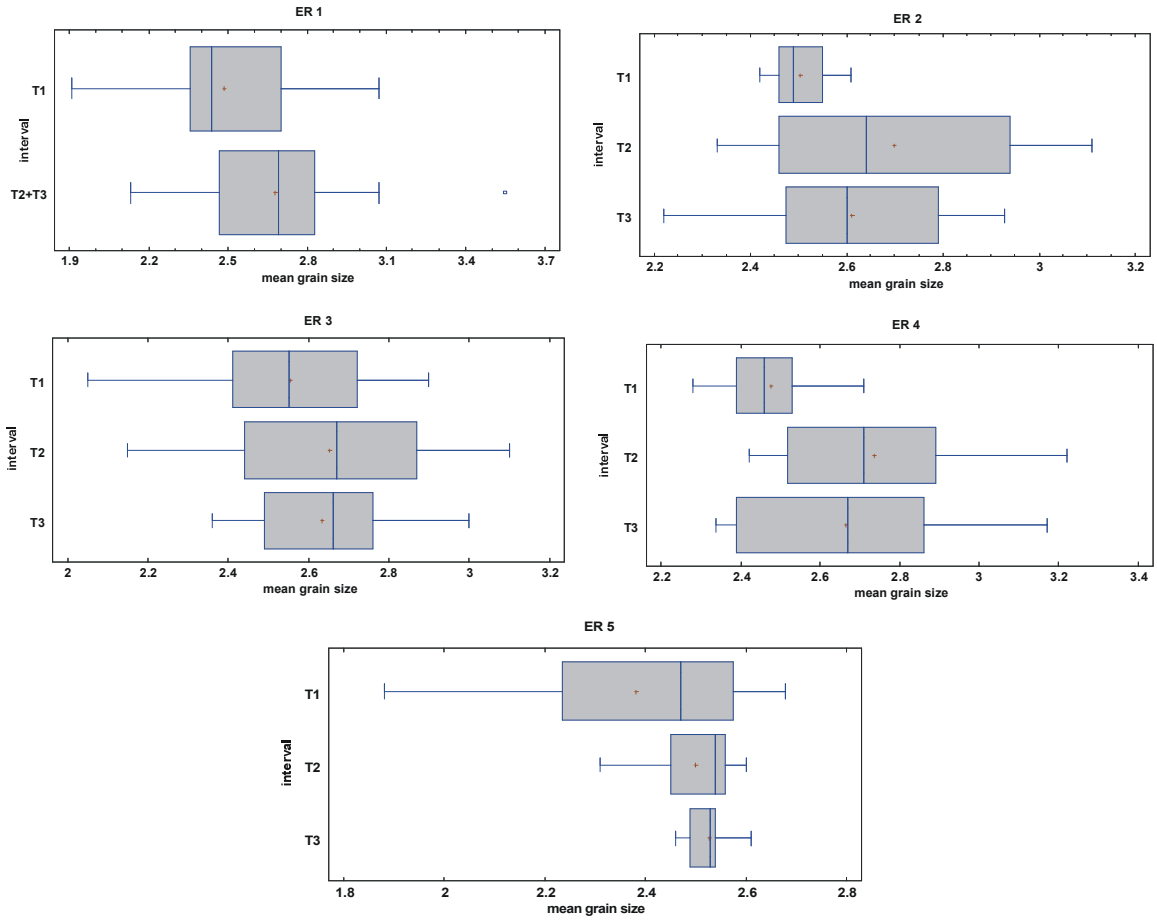

Fig. 10: Sediments mean grain size distributionamong East Rosetta profiles ER 1, ER 2, ER 3, ER 4 and ER 5 over different time spans

involves radioactive atoms of ^{238}U and ^{232}Th [30]. Both have radioactive series and emit alpha, beta and gamma radiation. They are responsible for the relative increase in the radioactive concentration of those samples. The results of the radioactivity were in agreement with the finding of El-Gamal and Saleh [31].

CONCLUSION

This study showed that, the Eastern side of the Rosetta Promontory has suffered from erosion during the whole 30 year-period and the highest average erosion rate reaching about -50 m/y at the promontory tip. The most intensive erosion (about – 137 m/y) occurred between 1985 and 1990, which is before the eastern revetment construction. The average accretion rate reached about 19 m/y during the 30 years' time period. On the other side, the Western Rosetta Promontory showed an average erosion rate during the whole period -15.5 m/y that was centered at the area down drift of the western revetment. The most intensive erosion rate at the western sector was between 1985 and 1990, which is before the western seawall construction. The horizontal shoreline retreat at the areas of the eastern and western seawalls has completely ceased after the seawall construction. While the erosion has been translocated to the lee sides of the constructions. The erosion rates reached around -20 m/y and -64 m/y at the lee sides of the western and eastern seawalls, respectively. This led to the construction of additional protective measures further to the west and east of the western and eastern seawalls respectively. These constructions were the nine groins in the western side and the five groins on the eastern side of the Rosetta Promontory. These structures have nearly ceased the erosion in situ, but it also translocated the erosion problem to its adjacent sides. The study also showed that there is a strong inverse relation between the mean grain size with both heavy minerals concentrations

and radioactivity. As the grain size decreases the proportion of heavy minerals and radioactivity increase. These factors occur on erosional sectors of the shoreline. This relation emphasizes the role of wave action in selective removal of the coarse, less dense minerals and settling in accretion sinks. This action enriches the fine denser minerals in erosion coasts, while concentrate them in accretion areas with coarse less dense minerals.

Recommendations: The coastal protection using hard structures is not the final process to mitigate erosion at coasts. So it is recommended to study the effect of Environmentally friendly soft structure for coastal protection (as sand nourishment and protective dunes) instead of hard structure or using both of them together. Also, further study is recommended for the effect of each protective structure through short and long term, assess its role in stabilizing the shoreline and study its negative impact on the neighborhood coastal area and its impact on the water quality and aquatic habitat. It is recommended to study different physical parameters of sediment (as magnetic property for example) as a new approach to distinguish between sediments from erosional or accretional beaches.

REFERENCES

1. Nielsen, E., 1976. Shore evolutions. Proc. Seminar Nile Delta Coastal Process, pp: 15-59.
2. Ghoneim, E., J. Mashaly, D. Gamble, J. Halls and M. Abu Bakr, 2015. Nile Delta exhibited a spatial reversal in the rates of shoreline retreat on the Rosetta promontory comparing pre- and post-beach protection. Geomorphology, 228: 1-14. doi:10.1016/j.geomorph.2014.08.021.
3. Shalash, S., 1982. Effects of sedimentation on the storage capacity of the High Aswan Dam reservoir. Hydrobiologia, 91: 623-639. doi:10.1007/BF00000061
4. UNESCO/UNDP. 1978. Coastal protection studies, final technical report.
5. Sestini, G., 1989. Nile Delta: A review of depositional environments and geological history. Geological Society, London, Special Publications, 41: 99-127. doi:10.1144/GSL.SP.1989.041.01.09.
6. Frihy, O.E., A.M. Fanos, A.A. Khafagy and P.D. Komar, 1991. Nearshore sediment transport patterns along the Nile Delta Egypt. Journal of Coastal Engineering, 15: 409.
7. Smith, E.S. and A. Abdel-Kader. 1988. Coastal erosion along the Egyptian Delta. Journal of Coastal Research, 4(2): 245-255.
8. Frihy, O.E. and K.M. Dewidar. 2003. Patterns of erosion/sedimentation, heavy mineral concentration and grain size to interpret boundaries of littoral sub-cells of the Nile Delta, Egypt. Marine Geology, 199: 27.
9. Aly, M.H., J.R. Giardino, A.G. Klein and H.A. Zebker, 2012. InSAR study of shoreline change along the Damietta Promontory, Egypt. Journal of Coastal Research, 284(5): 1263-1269. doi:10.2112/JCOASTRES-D-11-00182.1.
10. Frihy, O.E., M.M. El-Banna and A.I. El-Kolfat, 2004. Environmental impacts of Baltim and Ras El-Bar shore-parallel breakwater systems on the Nile delta littoral zone, Egypt. Environmental Geology, 45(3): 381-390. doi:10.1007/s00254-003-0886-y.
11. Dewidar, K.M. and O.E. Frihy, 2010. Automated techniques for quantification of beach change rates using Landsat series along the North-eastern Nile Delta, Egypt. Journal of Oceanography and Marine Science, 1: 28-39.
12. Deabes, E., 2017. Applying ArcGIS to Estimate the Rates of Shoreline and Back-Shore Area Changes along the Nile Delta Coast, Egypt. International Journal of Geosciences, 8: 332-348. doi:10.4236/ijg.2017.83017.
13. Frihy, O.E., E.A. Deabes and W.R. El-Sayed, 2003. Processes reshaping the Nile delta promontories of Egypt: pre- and post-protection. Journal of Geomorphology, 53(3): 263-279. doi:10.1016/S0169-555X(02)00318-5.
14. Elsayed, M.A.K., N.A. Younan, A.M. Fanos and K.H. Baghdady, 2005. Accretion and erosion patterns along Rosetta Promontory, Nile Delta Coast. Journal of Coastal Research, 21(3): 412.
15. Elsayed, M.A.K. and S. Mahmoud, 2007. Groins system for shoreline stabilization on the east side of the Rosetta Promontory, Nile Delta coast. Journal of Coastal Research, 23(2): 380-387. doi:10.2112/04-0319.1.
16. El-Banna, M.M., 2007. Erosion and accretion rates and their associated sediment characters 5 along Ras El Bar coast, northeast Nile Delta, Egypt. Environmental Geology, 52(1): 41-49. 6 doi:10.1007/s00254-006-0447-2.
17. El-Sayed, W.R., M.A. Aly, M.M. Iskander and A.M. Fanos, 2007. Evolution of Rosetta Promontory during the last 500 years , Nile Delta coast , Egypt. Eighth International Conference on the Mediterranean Coastal Environment. MEDCOAST 07, 2: 1003-1015.

18. CoRI/UNESCO/UNDP, 1978. Coastal Protection Studies, Final Technical Report.
19. Fanos, A.M., A.A. Khafagy and R.G. Dean. 1995. Protective works on the Nile Delta coast. Journal of Coastal Research, 11(2): 516-528.
20. Ghoneim, E., 2009. A Remote Sensing Study of Some Impacts of Global Warming on the Arab Region. Climate Change: The Arab Forum for Environment and Development (AFED).
21. Fanos, A.M., 1999. Problems and protection works along the Nile delta coastal zone. Fifth International Conference on Coastal and Port Engineering in Developing Countries.
22. Frihy, O.E. and M.F. Lotfy, 1994. Mineralogy and textures of beach sands in relation to erosion and accretion along the Rosetta Promontory of the Nile Delta, Egypt. Journal of Coastal Research, 10(3): 588-599.
23. El-Gamal, A., 2012. New approach for erosion and accretion coasts discrimination. Journal of Coastal Research, 389-398. doi:10.2112/JCOASTRES-D-10-00154.1
24. Frihy, O.E., S.M. Shereet and M.M. El-Banna, 2008. Pattern of beach erosion and scour depth along the Rosetta Promontory and their effect on the existing protection works, Nile Delta, Egypt. Journal of Coastal Research, 24(4): 857.
25. Xu, H., 2006. Modification of Normalised Difference Water Index (NDWI) to enhance open water features in remotely sensed imagery. International Journal of Remote Sensing, 27(14): 3025-3033. doi:10.1080/01431160600589179.
26. Kelly, J.T. and A.M. Gontz, 2018. Using GPS-surveyed intertidal zones to determine the validity of shorelines automatically mapped by Landsat water indices. International Journal of Applied Earth Observation and Geoinformation. 65: 92-104. doi:10.1016/j.jag.2017.10.007.
27. Krumbein, W.C. and F.J. Pettijohn, 1938. Manual of sedimentary petrography. D. Applenton-Century Company.
28. International, S.E.I., 2014. Inspector USB Manual.
29. El-Asmar, H.M. and K. White, 2002. Changes in coastal sediment transport processes due to construction of New Damietta Harbour, Nile Delta, Egypt. Coastal Engineering, 46: 127.
30. El-Gamal, A.A., 2014. Assessment of Natural Radioactivity Distribution in Surface Sediments at Erosion and Accretion Sites of Nile Delta Coastal Profiles, Egypt. International Journal of Marine Science, 4(36): 1-12.
31. El-Gamal, A.A. and I.H. Saleh 2012. Radiological and mineralogical investigation of accretion and erosion coastal sediments in Nile Delta region, Egypt. Journal of Oceanography and Marine Science, 3(3): 41-55.